Tr. J. of Physics
23 (1999) , 463 – 469.

The Experimental Studies on Zr Photoelectron Spectra

I. BURIBAYEV, N.A. NURMATOV, N. TALIPOV
Physics Faculty, Tashkent State University.
The Republic of Uzbekistan

Received 25.09.1995

Abstract

Photoelectron spectra (PES) taken from crystalline Zr at 8.4 eV and 10 eV have been studied by a high resolution photoelectron analyzer, with ΔE=0.1 eV, and the results were compared to the results calculated for electron density of states in the valence band. Photoelectron work function (WF) measured from the atomically clean Zr surface by Fowler isothermal curves was found to be 3.95 eV $\pm$ 0.02 eV. It was shown that a small dose of residual gas, namely CO, absorbed on the Zr surface, resulted in a decrease of the WF by 0.15-0.25 eV as well as a variation in the PES.

Introduction

Zr is often used as an alloy component for refractory metals. And approximately 1% of Zr is found to be sufficiently present in the alloys in order to cover its surface with a thin film under alloy baking. Moreover, Zr is active with gases such as carbon, hydrogen, oxygen and thus easily forms carbides, hydrides and oxides.

There exist a few works [1,2] that have explored Zr photoelectron parameters, but these experiments had been performed under low vacuum and without controlling the surface composition with independent methods. The WF values reported had a very large spread, from 3.7 eV to 4.33 eV. For Zr films produced by thermal evaporation under high vacuum its value was equal to 4.05 eV $\mp$ 0.1 eV [3]. That, these WF values had been measured to within 0.1 eV indicates there were uncontroled variations in both the chemical composition and structure of the Zr films. Hence, in order to unambiguously interpet the Zr photoemission parameters, it is necessary establish strict vacuum conditions as well as purification and control processes.

The purpose of the investigation reported here is (i) to produce a atomically clean Zr surface, (ii) to evaluate Zr photoelectron parameters and PES, and (iii) to specify factors influencing PES.

Experiment

Zr specimens were cut from a large crystal using a diamond disc. The crystals obtained were mechanically polished and chemically etched. They were of 8-mm diameter and 1.5-mm thick. Then these specimens were mounted on a cathodic assembly and installed into an manipulator apparatus. Experimental setup and technique has been described elsewhere [4,5].

Baking of the specimens have been performed as follows. Crystal temperature was raised gradually in steps of 100°C after which a prolonged heating was carried out at temperatures between 1700 K and 1950 K. During this process, variation in chemical composition of the specimen surface was monitored via Auger spectra taken under both the heating and at room temperature. In all, the crystals were heated for more than 70 h and their temperatures were monitored by a WRe 5/20 thermocouple. Strong evaporation of Zr atoms takes place when crystal temperature raises to 1900 K and higher.

Auger spectra have subsequently shown Zr carbide was not completely removed, its traces still present on the crystal surface. Prolonged baking for 20-30 min. with a controled oxygen leak-in followed by larse temperature enhancement to 1900K-1950K, multiply repeated in alternate sequence, resulted in efficient purification of the surface from Zr carbide. In Fig.1 we can see that all the intensive peaks located in the range of 50eV-300eV are well defined. Vacuum in the experimental chamber was held at 2×10^{-10} Torr with the Auger analyzer gun having its cathode switched on. Test photoemission measurements were carried out at 5×10^{-11} Torr.

Results

Spectral dependence of photoemission quantum yield has been measured from atomically clean Zr surface at photon energies 4eV to 5.2 eV. Zr WF was measured by the Fowler method [6] and was equal to 3.95 eV$\pm$0.02 eV. Its WF value decreased to 3.80 eV-3.75 eV after baking the specimen for 20-25 min. A carbon peak appears in the Auger spectrum (see Fig.1b). Therefore, every 25 min the specimens were heated by interval at 1700K-1800K.

In Fig 2., two photoelectron energy distribution curves (EDCs) are plotted at 8,4 eV (1) and 10 eV (2), respectively, as measured from the Zr surface. We can see that with the photon energy increase the high-energy edge is shifted to the higher energies by an amount which corresponds to the photon energy increase. Maxima in the low-energy part are not shifted and with the photon energy increase their amplitudes increase as well. Also, with the photon energy increase, maxima in the high-energy part of this spectrum are shifted.

In Fig 3. Zr density of states (a) [7], EDCs soluting curves (b) and experimentaly determined curves of EDC versus energy (c), with respect to the initial energies are plotted. On the abscissa the energy, in eV, and the Fermi level are situated. According to Fig. 3, with photon energy increase from 8.4 eV to 10 eV, the maxima locations of peaks (B and C) are invariable. At 0.3eV-0.5eV below the Fermi level, a weak maximum (A) appears. At 8.4 eV this maximum is manifested as a step, where the amplitude

increases with the photon energy to 10 eV. Peak D is observable in a low-energy part being located on the slope of the low-energy maximum induced by the energy losses due to electron-electron collisions.

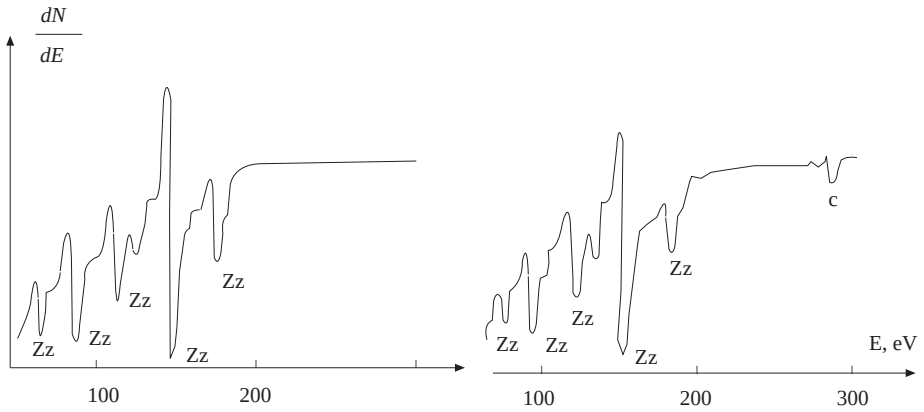

a). for atomically clean surface; **b)** after 25 min upon completion at baking

Figure 1. The Auger spectra taken from the Zr specimen surface:

In the photoemission model, where indirect optical transitions are predominant, maxima induced by electron density of states exhibit constant positions [8,9] with respect to the photon energy. Such is the case for Zr PES peaks B,C in Fig. 3b.

By using the indirect model, with the assumptions taken from [8,9] for photoelectron energy-distribution function, we can derive the following relation:

$$N(E)dE = const T(E)\rho(E)\rho(E - h\nu)dE, \tag{1}$$

where T(E) is the yield function and ρ(E) and $\rho(E - h\nu)$ are the initial and excited density of states, respectively. In [10], an expression for T(E) is given in a simple model of isotropic electron velocity distribution:

$$T\langle E\rangle = 0.5[1 - \sqrt{E_F + e\Psi/E_F + e\Psi + E}], \tag{2}$$

where E_F is the Fermi energy, $e\varphi$ is the photoelectron WF, and E is photoelectron energy.

Here, Eq.1 permits to calculate photoelectron EDCs from electron densitity of states ρ(E), evaluated for the valence band of a metal. We take ρ(E) as being calculated for Zr in [7] (Fig. 3a).

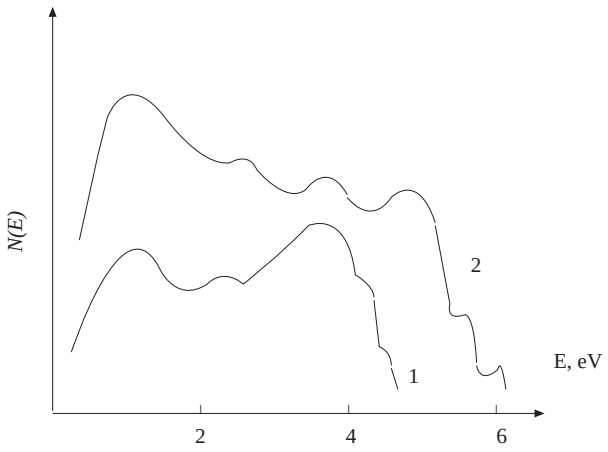

Figure 2. Photoelectron EDCs plotted for the Zr atomically clean surface at 8.4 eV and 10eV (curve 1 and 2, respectively).

The results calculated for electronic structure of Zr valence band as well as an energy distribution of electron density of states have been reported by Jepsen et al. [7] and Loucks [11], who demonstrated that at 0.95 eV and 2.3eV below the Fermi level there are two maxima within the filled band. These maxima reflect largerly the d-band structure. S-and p-electrons make a small contribution to the second maximum in the density of states.

The schema for the N(E) calculation is described in [10]. Figure 3b shows photoelectron EDCs calculated at 8.4 eV and 10 eV (curves 1 and 2, respectively). In calculated spectra two maxima are connected by electron density of states. The calculated curves, N(E), compared to the experimental PES (see Fig. 3 c), have shown that maxima B,C at 1.1 eV and 2.5 eV below the Fermi level are connected by the density of states in the Zr filled band.

In the photoelectron PES of fig. 3c, we see two additional peaks (A,D) which are sensitive to residual gas. Figure 4 shows N(E) plotted at 10 eV for both the Zr atomically clean surface (curve 1) and for its surface having carbon traces (curve 2) which are observable in Auger spectra (Fig. 1b). In this figure, the low-energy maximum amplitude increases and both peaks (A,D) disappear. This indicates a surface origin for the above peaks. The study of Zr polycrystalline specimens made it difficult to recognize contributions from direct transitions, and thus were not observable in PES. Visual inspection of the specimen surface after it was removed from the experimental chamber demonstrated the very granular structure (0.1mm-0.5mm) even after such prolonged heating. Hence, we may conclude that all crystallographic directions outlined on the specimen surface make their contributions to photoelectron PES.

Conclusions

1. The process of thermal purification of the Zr specimen surface from various impurities, such as oxygen, carbon and sulphur, has been investigated along with simultaneous control of variations in element composition by the AES method. Zr carbide is shown to be removed from the specimen surface by means of both oxidation and high-temperature heating (1800K-1950K), being repeated in alternate sequence.

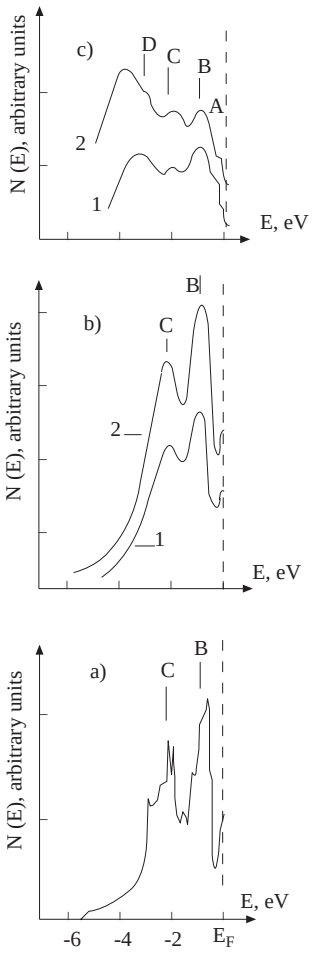

Figure 3. a) Calculated Zr state density [7]. b) Zr photoelectron EDCs calculated at $e\varphi$=3.95 eV, $h\nu$=8.4 eV (curve 1), and $h\nu$=10 eV (curve 2). c) Photoelectron EDCs plotted for the Zr atomically clean surface at 8,4 eV (1) and 10 eV (2) versus the Fermi level.

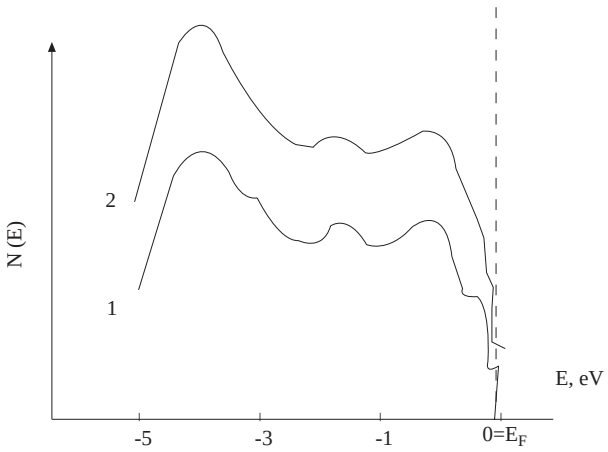

Figure 4. Experimental Zr photoelectron EDCs plotted at $h\nu$=10eV: a)- before the residual gas is absorbed (curve 1), and b) after absorption (curve 2).

2. Spectral dependence of quantum yield has been measured in order to evaluate photoelectron WF, which was equal to 3.95 eV±0.02 eV and was found to be decreased by 0.15 eV - 0.25 eV for Zr surface due to the residual gas adsorption.

3. When comparing the calculated photoelectron EDCs to the experimental PES. we refer to the observable maxima B, C as an electron density of states for the Zr filled band.

4. It has been demonstrated that for an atomically clean Zr surface the surface-sensitive maxima were found in PES, and disappeared due to residual gas adsorption.

5. The maximum amplitude induced by photoelectron inelastic energy losses increases with the photon energy increase.

The above results may be used in the analysis of electron structure when it is calculated for transition metals, such as Zr., and may prove to be useful for the interpretation of Zr emissive, adsorptive, and catalytic properties as well as Zr-containing alloys of transition metals.

References

[1] H. Rentschler, D. Henry, K. Smith, Rev.Sci. Instrum., vol.3 N 12 (1932) 794-802.

[2] H. Malamud and A. Krumbein, J.Appl. Phys., vol.25, N5 (1954) 591-592.

[3] D.E. Eastman, Photoelectric work Functions of Transition, Rare-Earth and Noble Metals. Phys.Rev.B.,vol.2, N1 (1970), p.1-2.

[4] I. Buribayev, N.A. Nurmatov, The photoemission from Nb single crystal and Nb-Mo alloy in the vacuum ultraviolet. IZV. Akad. SSSR, Ser.Fiz. vol.55, N12, (1991), 2450-2454.

[5] I. Buribayev, N.A. Nurmatov, UV photoelectron spectra of Nb and Mo single-crystal surfaces. Journ.of Electron Spectroscopy and Related Phenomena vol.68, (1994) 547-554.

[6] A.L. Hughes and L.A. DuBridge, Photoelectric phenomena Mcgraw-Hill Book, Company, INC NEW YORK and LONDON, 1932.

[7] O. Jepsen, O. Krogh Andersen, A.R. Mackintosh, Electronic structure of hcp transition metals. Phys. Rev.B. vol. 12, N 8 (1975), 3084.

[8] C.N. Berglund, W.E. Spicer, Photoemission studies of Copper and Silver: Theory. Phys.Rev., vol.136, N4A, (1964) 1030.

[9] C.N. Berglund, W.E. Spicer, Photoemission studies of Copper and Silver: Experiment. Phys.Rev., vol.136, N4A, (1964) 1044.

[10] B.B. Shishkin, I. Buribayev, Photoelectron emission of nonuniform objects. Radiotechnica and Electronica, vol. 19, N9, (1974) 1948-1954.

[11] T.L. Loucks, Electronic Structure of Zirconium. Phys.Rev., vol.159, N3, (1967). 544-551.